Nucleation and growth of ZnO nanorods on the ZnO-coated seed surface by solution chemical method

Juan Zhao [*], Zheng-Guo Jin, Tao Li, Xiao-Xin Liu

Key Laboratory for Advanced Ceramics and Machining Technology of Ministry of Education, Tianjin University, Tianjin 300072, China

Abstract

ZnO nanorods on ZnO-coated seed surfaces were fabricated by solution chemical method using supersaturated $(ZnNO_3)_2$/NaOH at 70 °C. The seed surfaces were coated on glass substrates by sol–gel processing, and their texture was dominated by heating temperatures, cooling styles and layer thickness per dipping. The effects of the seed surface on the morphology of the resultant nanorods were primarily discussed. The orientation and morphology of both the seed surface and successive nanorods were analyzed by using XRD and SEM. It is proved that when the seed size increases from 15 to 50 nm with temperature increasing, the average diameter of the resultant nanorods increase from 25 to 50 nm, with a length of 800 nm after growing for 1.5 h. The seed surface prepared by heating at 300–400 °C, fast cooling or drawing at lower speed has better orientation and few surface defects, which leads to higher density of nuclei on the seed surface and thus to the optimal preferred crystal growth of ZnO rods standing perpendicular onto substrates.
© 2005 Elsevier Ltd. All rights reserved.

Keywords: ZnO; Nanorod; Interfaces; Grain growth

1. Introduction

ZnO nanomaterials have been widely studied for a variety of high-technology applications ranging from surface acoustic wave filters,[1] photonic crystals,[2] light-emitting diodes,[3] photodetectors,[4] photodiodes,[5] optical modulator waveguides,[6] varistors[7] to gas sensors,[8] due to its wide bandgap, excellent chemical and optoelectronic properties as a II–VI semiconductor with a large excition binding energy. Recently, photovoltaic devices like solar cells based on bare[9] and dye-sensitized thin films[10–12] have shown great potential of ZnO for such applications. It is known that an important approach to improve the efficiency of photoelectric conversion of the nanocrystallite solar cells is to build single crystalline and columnar semiconductor electrodes with high orientation and a high specific area, which are expected to improve the separation of electron-hole pairs photogenerated and their transportation.[13] Hitherto, various techniques have been successful in creating highly oriented ZnO nanorods, such as molecular beam epitaxy, radio frequency magnetron sputtering,[14] metalorganic chemical vapor deposition,[15] spray pyrolysis[16] and pulsed laser deposition.[17] But many of them demand stringent reaction conditions such as high temperature and low or high pressure, which go against large-scale production of this material. More recently, solution methods such as cathodic electrodeposition,[18] thermal decomposition,[19] and the use of complexing agents[20] have been used as low cost, moderate methods to produce ZnO nanorods. Particularly, a bottom-up hydrothermal synthesis approach proposed by Vayssieres[19,21,22] do not require any template, membrane, surfactant or applied external field to create nanorods with good orientation.

The obvious preferred orientation of ZnO along [0 0 1] is closely related to its crystal structure, which consists of a nonpolar plane ($\bar{1}$ 0 0) with C_{6v} symmetry, a polar basal oxygen plane (0 0 $\bar{1}$), and a polar top face (0 0 1) comprised of tetrahedral zinc having a terminal OH ligand.[21] The low-

* Corresponding author. Tel.: +86 22 27890266; fax: +86 22 27404724.
  E-mail address: tonyjane666@yahoo.com.cn (J. Zhao).

symmetry, nonpolar ($\bar{1}\,0\,0$) face is the most stable, while the polar faces with high surface energy are metastable. Therefore, the most stable morphology is hexagonal with the crystal elongated along the c-axis. The nucleation and growth of ZnO nanorods on substrates in aqueous environment have been discussed previously by Vayssieres.[19,21,22] Vayssieres emphasized that controlling the interfacial tension is the key to control the shape and the orientation of crystallites growing on a substrate. In fact, the interfacial tension is strongly dominated by various factors, like the crystal orientation of the seed surface and defects on it. In this paper, we employ an aqueous solution containing NaOH and $Zn(NO_3)_2$ and substrates coated with ZnO as seeds through sol–gel processing for ZnO rod deposition. The effects of crystal orientation and defects of the coated ZnO seed surface on the relationship between nucleation and growth of the resultant nanorods were primarily explored by changing heating temperature, cooling style and coated-film quality when preparing the seed surface.

2. Experimental procedure

Fig. 1 shows the flow chart of the preparation of the seed surface. $Zn(CH_3COO)_2 \cdot 2H_2O$ (0.75 mol/l) was first dissolved in a 2-methoxyethanol-monoethanolamine(MEA) solution (0.75 mol/l) at room temperature. The resultant solution was stirred at 60 °C for 30 min to yield a clear and homogeneous solution. Then a clean glass substrate was dipped into the solution, and withdrawn at various speeds (WS). Finally, the as-coated substrate was heated in the electrical furnace at different temperatures for 10 min and cooled in two styles: one is cooling the samples to RT in the furnace (slow cooling); the other is drawing the samples out of the furnace and keeping them in the air (fast cooling). Table 1 shows the processing parameters for the seed surface. The ZnO-coated substrates were rinsed with deionized water, and then suspended in an aqueous solution of 0.001M $(ZnNO_3)_2$/0.1 M NaOH stirred
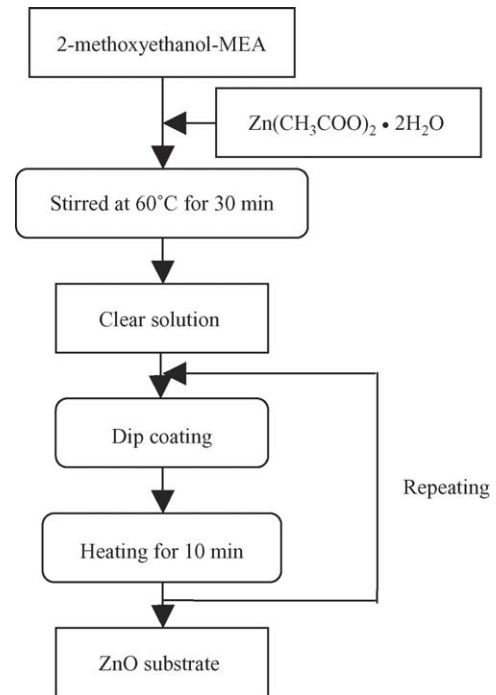

Fig. 1. The flow chart showing the procedure for preparation of seed surfaces.

Table 1
The preparation conditions for the seed surface

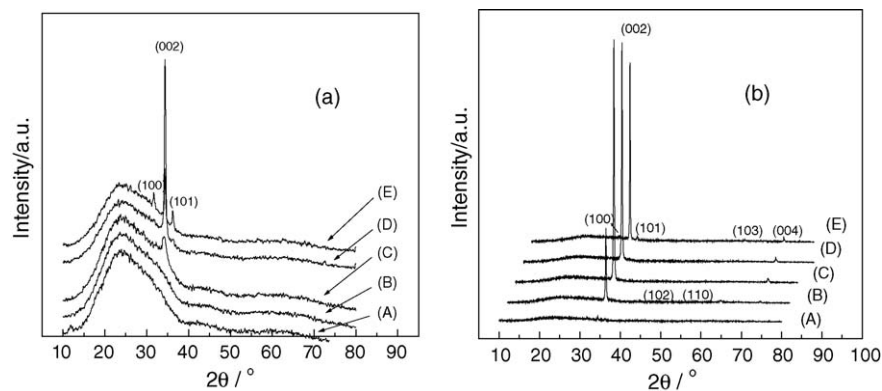| WS (cm min^{-1})	Heating temperature (°C)	Cooling style	Dipping times
3.5	100	Fast	3
3.5	200	Fast	3
3.5	300	Fast	3 and 6
3.5	400	Fast	3
3.5	500	Fast	3
1.2	300	Fast	5
7.0	300	Fast	2
3.5	300	Slow	3 and 6

Fig. 2. XRD patterns of the ZnO seed surface (a) and nanorods (b). (The seed surface was prepared by repeating the dip coating-heat treatment-fast cooling process three times. The heating temperatures were 100 °C (A), 200 °C (B), 300 °C (C), 400 °C (D), 500 °C (E) and WS was 3.5 cm/min.)

over a hot plate at 70 °C for 1.5 h. The resultant samples were rinsed with deionized water and dried in the air.

XRD patterns of the seed surface and resultant nanorods was measured on a Rigaku 2500 X-ray diffractometer with Cu Kα radiation ($\lambda = 1.54056$ Å) at 40kV/150 mA in a continuous scan from $2\theta = 10$ to $80°$. The FE-SEM images of the seed surface and resultant nanorods were observed by a JEOL JSM6700 microscope.

3. Results and discussion

3.1. Effects of heating temperatures

Fig. 2 shows XRD patterns of the ZnO seed surfaces with different heating temperatures and of the resultant nanorods. The heating temperatures were 100–500 °C, WS was 3.5 cm/min, and the seed surface was prepared
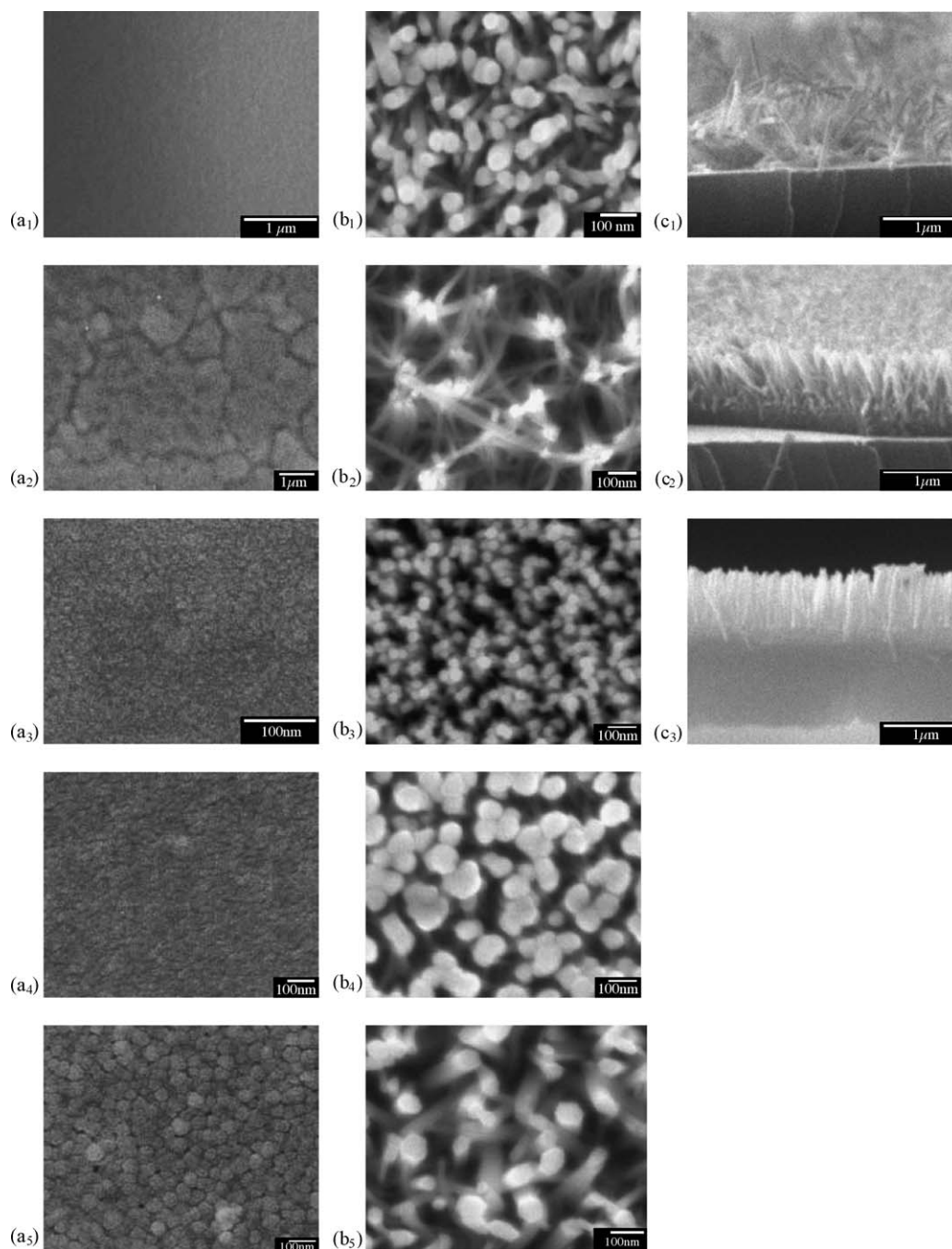

Fig. 3. SEM photographs of the ZnO seed surfaces (a) and nanorods (b). (The seed surface was prepared by repeating the dip coating-heat treatment-fast cooling process three times. WS was 3.5 cm/min, and annealing temperatures were 100 °C (a_1), 200 °C (a_2), 300 °C (a_3), 400 °C (a_4), 500 °C (a_5). The cross section of (b_1)–(b_3) are (c_1)–(c_3).)
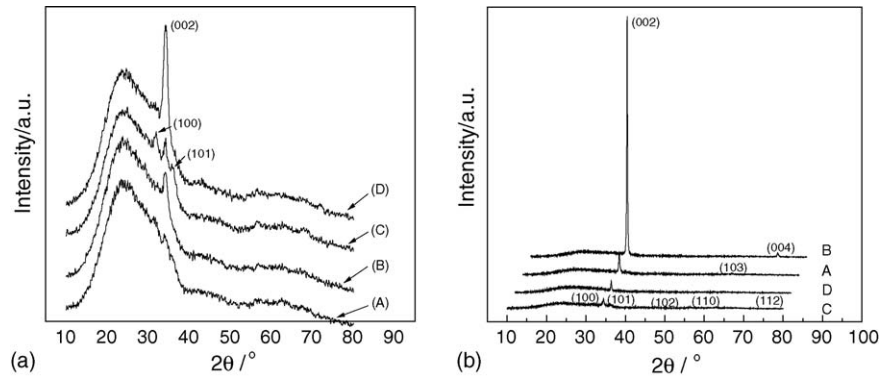
Fig. 4. XRD patterns of the ZnO seed surface (a) and ZnO nanorods (b). (The seed surface was prepared by the dip coating (WS = 3.5 cm/min)-heat treatment (300 °C)-cooling process. (A) Repeating the process three times with slow cooling, (B) Repeating the process three times with fast cooling, (C) Repeating the process six times with slow cooling, (D) Repeating the process six times with fast cooling.)

by repeating the dip coating-heating-fast cooling process three times. It can be seen from (a) that the protruding background originates from the glass substrate. No narrow peak can be seen below 300 °C, indicating that ZnO seed particles are still amorphous. The peak intensity of the (0 0 2) plane of ZnO appears from 300 °C and becomes stronger in the order of the heating temperature 500 < 300 < 400 °C, suggesting that heating at 400 °C gives the highest degree of crystal orientation for the seed surface. Fig. 2(b) exhibits that the peak intensity of the (0 0 2) plane of the corresponding nanorods increases with increasing temperature at below 300 °C, indicating that the degree of crystal orientation increases with increasing temperature. The peak intensity of the nanorods above 300 °C decreases with increasing temperature, indicating that heating at 300 °C provides optimal preferred crystal orientation for nanorods.

The thermal decomposition temperature of the zinc acetate is 240 °C[23] and the crystallization of ZnO prepared from zinc acetate-2-methoxyethanol-MEA solutions begins at 200–300 °C,[24] and so ZnO particles in the seed substrate are not crystallized completely below 300 °C. During 300–400 °C, the fact that with increasing temperature, the degree of orientation of the seed surface along the polar plane (0 0 2) increases may be attributed to the rearrangement of ions, which can satisfy the decrease of the free energy of the polar (0 0 2) plane. When the heating temperature is elevated up to 500 °C, the crystal particles grow bigger, disturbing the unidirectional crystal growth and leading to the lower degree of orientation along c-axis. Since the rods tend to grow epitaxially in term of the orientation of the ZnO seeds, their dependence of orientation upon heating temperatures above 300 °C should be the same as that of the seeds. However, the optimal orientation is 400 °C for the seeds and 300 °C for the rods. The difference may be attributed to the poor chemical activity of the seed face at 400 °C, which causes the decreasing density of nuclei and thus lower degree of the crystal orientation at 400 °C.

Fig. 3 is SEM photographs of the ZnO seed surface with different heating temperature and resultant nanorods. The preparation condition is the same as that mentioned in Fig. 2. It is seen from (a) that the seed surface heated at 100 °C is smooth, the one heated at 200 °C has shallow defects like ravine, and the ones heated at above 300 °C are smooth again. The grains become clearer to be seen and their size increases. The average diameters of grains are 15, 25 and 50 nm for 300, 400 and 500 °C, respectively. Fig. 3(b) and (c) show different morphology of nanorods. At 100 °C, rods show flower shape; at 200 °C, rods tend to slope; at 300–400 °C, rods stand perpendicular onto substrates; at 500 °C, rods again incline. The different morphology can be explained in this way: at 100 °C, crystallization and orientation of the seed surface have not begun. The vaporization of the solvents is in the initial stage, and brings the smooth surface, so the density of nuclei on the substrate is low. The system will thus promote the stretched epitaxial growth of the rods along c-axis from a limited number of nuclei, which induces a star-shape (or flower-shape) morphology. When it comes to 200 °C, the degree of orientation of the seed surface increases, but the vaporization and decomposition of the solvents are more obvious, giving the texture of defects like ravine. Under this condition, the density of nuclei is lower, and the resultant rods slant to each other. Above 300 °C, the particles on the substrate crystallize, rearrange, and orientate, accompanying the healing of defects like ravine. Correspondingly, the good orientation and the decreasing defects on the seed surface make the density of nuclei increase notably. This will allow the slow growth along the easy direction of crystallization, and generate a condensed phase of anisotropic nanorods parallel to the substrate normal. At 500 °C, the obvious growth of crystallites on the seed surface leads to the decreasing of the degree of orientation as mentioned above. Therefore, the density of nuclei decreases again, resulting in the incline of grown rods. In addition, it can be seen from Fig. 3(b) and (c) the diameters of the nanorods are ~30, 25, 25, 25 and 50 nm for 100–500 °C, and their lengths are about 800 nm. The diameter of nanorods is found to increase according to the size of crystal seeds.
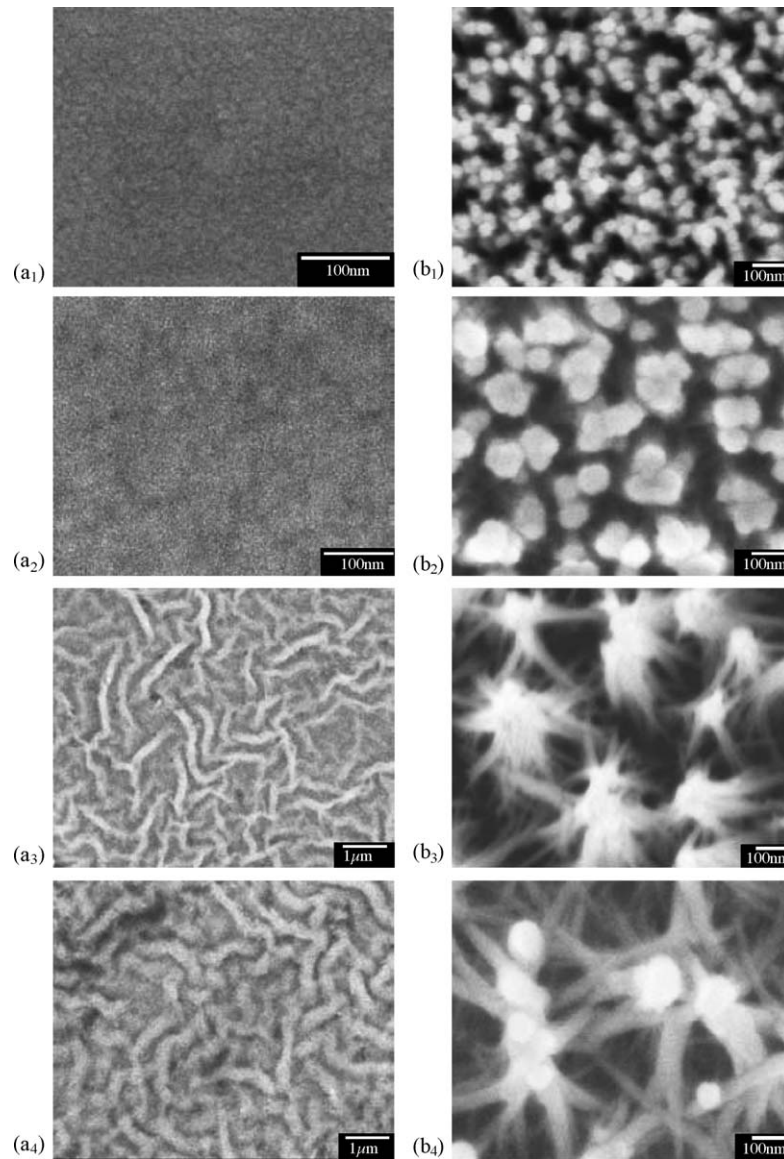
Fig. 5. SEM photographs of the ZnO seed surface (a) and ZnO nanorods (b). (The seed surface was prepared by the dip coating (WS = 3.5 cm/min)-heat treatment (300 °C)-cooling process. (a_1) Repeating the process three times with fast cooling, (a_2) Repeating the process six times with fast cooling, (a_3) Repeating the process three times with slow cooling, (a_4) Repeating the process six times with slow cooling.)

3.2. The effects of cooling styles

Fig. 4 shows XRD patterns of the ZnO seed surface with different cooling styles and resultant nanorods. The heating temperature was 300 °C, WS was 3.5 cm/min, and the seed surface was prepared by repeating the dip coating-heat treatment-cooling process for both three and six times. It can be seen that for both three and six times, the peak intensity of (0 0 2) plane of the seed surface prepared by fast cooling is higher than that prepared by slow cooling, indicating that the degree of crystal orientation of (0 0 2) plane is enhanced by fast cooling. Meanwhile, the same change can be found for ZnO rods, which are a continuation of the substrate grain. Fig. 5 is SEM photographs of the ZnO seed surface with different cooling styles and resultant nanorods. The preparation condition is the same as that mentioned in Fig. 4. It shows that the seed surface prepared by fast cooling has evenly distributed crystallites and few defects; the density of resultant nanorods is high and ZnO rods stand completely perpendicular onto substrates. While the domain like striation form on the seed surface prepared by slow cooling, and corresponding nanorods incline to different extent.

These results indicate that during fast cooling, the surface state with high orientation of (0 0 2) and few microstructure defects is kept the same as that at 300 °C (Fig. 3(a_3)). This causes higher density of nuclei on the seed surface and the rods exhibit in a perpendicular fashion by crowding among a number of bar crystallites. While during slow cooling, there is enough time for ions to aggregate along the crystal planes having similar lattice match in order to decrease
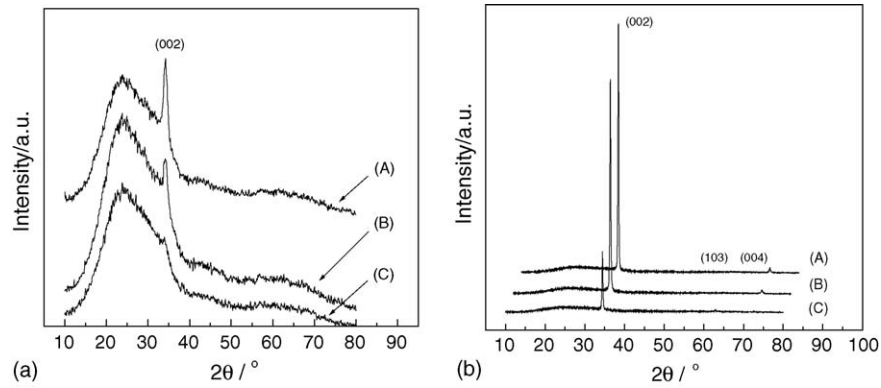
Fig. 6. XRD patterns of the ZnO seed surface(a) and ZnO nanorods (b). (The seed surface was prepared by repeating the dip-coating at WS of 1.2 cm/min (A), 3.5 cm/min (B) and 7.0 cm/min(C) five, three and two times, respectively. The heat-treatment is at 300 °C and in fast cooling style.)
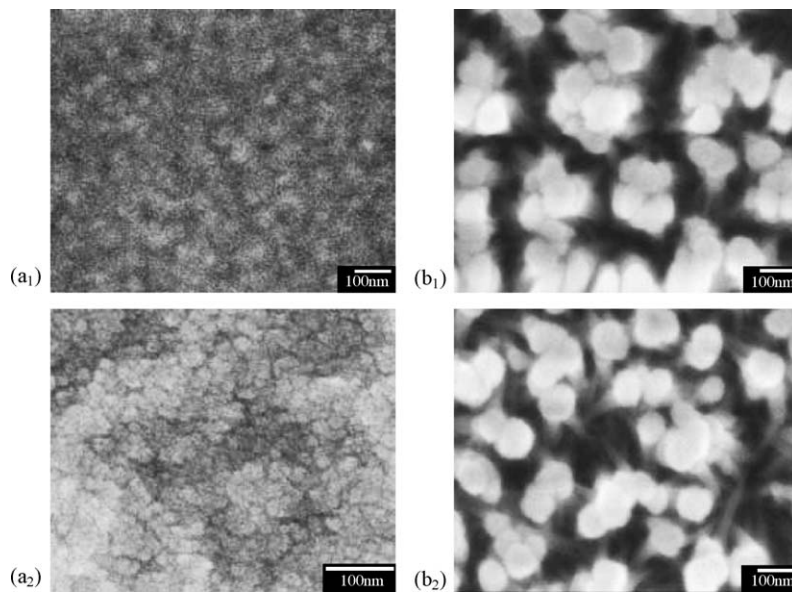

Fig. 7. SEM photographs of the ZnO seed surface (a) and ZnO nanorods (b). (The seed surface was prepared by repeating the dip-coating at WS of 1.2 cm/min (a_1) and 7.0 cm/min (a_2) five and two times, respectively. The heat-treatment is at 300 °C and in fast cooling style.)

their high surface energy. This process produces the domain like striation(Fig. 5(a)), and partly destroys the preferred orientation along (0 0 2) plane and the uniformity of the seed surface, which results in the low density of nuclei and the rod growth style of inclination.

3.3. The effects of layer thickness per dipping

Fig. 6 shows XRD patterns of the ZnO seed surface with different layer thickness per dipping (versus different drawing speeds) and resulting nanorods. The seed surface was prepared by repeating the dip-coating at WS of 1.2 cm/min (~200 nm/dipping), 3.5 cm/min (~300 nm/dipping) and 7.0 cm/min (~500 nm/dipping) five, three and two times, respectively. The heat-treatment was at 300 °C and in fast cooling style. The number of dipping was selected to attain the film thickness of about 1 μm at a given WS. The peak intensity of (0 0 2) of seed surface is found to increase with

decreasing WS. A possible reason is that when the layer thickness per dipping is thin, the solvent more easily evaporate, the seed surface is denser and has few defects. Further, this leads to better orientation (Fig. 6(a)) and higher density of nuclei (Fig. 7(a)) of the seed surface, and the homogenization of nanorod arrays improves (Fig. 7(b)).

4. Conclusion

In the system of $(ZnNO_3)_2$/NaOH solution, the texture of the ZnO seed surface has great effects on growth of resultant nanorods, whose morphology primarily depends on the density of nuclei restricted by the crystal orientation and surface defects of the seed plane. When heating temperature is below 300 °C, the seeds have not crystallized completely, and the poor orientation of the seed surface lead to low density of nuclei and lodging of nanorods. When at 300–400 °C,

the seed surface has high orientation and few defects, which result in high density of nuclei and perpendicular standing of nanorods. When at 500 °C, the further growth of seed grains causes the decrease of orientation, so the density of nuclei reduces again and nanorods incline to each other. Meanwhile, with increasing temperature, the size of seeds increases and the diameter of resulting nanorods increase from 25 to 50 nm. In addition, the fast cooling style makes for retaining good orientation of the seed surface under high temperature; the thinner layer per dipping contributes to uniformity of the seed surface. Both of them give high density of nuclei and make ZnO rods grow unidirecionally in a crowded environment and stand perpendicular onto substrates.

Acknowledgement

References

1. Emanettoglu, N. W., Gorla, C., Lio, Y., Liang, S. and Lu, Y., Epitaxial ZnO piezoelectric thin films for SAW filters. *Mater. Sci. Semicond. Process.*, 1999, **2**, 247–252.
2. Chen, Y., Bagnall, D. and Yao, T., ZnO as a novel photonic material for the UV region. *Mater. Sci. Eng. B*, 2000, **75**, 190–198.
3. Saito, N., Haneda, H., Sekiguchi, T., Ohashi, N., Sakaguchi, I. and Koumoto, K., Low-temperature fabrication of light-emitting zinc oxide micropatterns using self-assembled monolayers. *Adv. Mater.*, 2002, **14**, 418–420.
4. Liang, S., Sheng, H., Liu, Y., Hio, Z., Lu, Y. and Shen, H., ZnO Schottky ultraviolet photodetectors. *J. Cryst. Growth*, 2001, **225**, 110–113.
5. Lee, J. Y., Choi, Y. S., Kim, J. H., Park, M. O. and Im, S., Optimizing n-ZnO/p-Si heterojunctions for photodiode applications. *Thin Solid Films*, 2002, **403**, 553–557.
6. Koch, M. H., Timbrell, P. Y. and Lamb, R. N., Influence of film crystallinity on the coupling efficiency of ZnO optical modulator waveguides. *Semicond. Sci. Technol.*, 1995, **10**, 1523–1527.
7. Lin, Y., Zhang, Z., Tang, Z., Yuan, F. and Li, J., Characterization of ZnO-based varistors prepared from nanometre precursor powders. *Adv. Mater. Opt. Electron.*, 1999, **9**, 205–209.
8. Golego, N., Studenikin, S. A. and Cocivera, M., Sensor photoresponse of thin-film oxides of zinc and titanium to oxygen gas. *J. Electrochem. Soc.*, 2000, **147**, 1592–1594.
9. Keis, K., Vayssieres, L., Rensmo, H., Lindquist, S.-E. and Hagfeldt, A., Photoelectrochemical Properties of Nano- to microstructured ZnO electrodes. *J. Electrochem. Soc.*, 2001, **148**, A149–A155.
10. Tennakone, K., Kumara, G. R. R. A., Kottegoda, I. R. M. and Perera, V. P. S., An efficient dye-sensitized photoelectrochemical solar cell made from oxides of tin and zinc. *Chem. Commun.*, 1999, 15–17.
11. Rensmo, H., Keis, K., Lindstrom, H., Sodergren, S., Solbrand, A., Hagfeldt, A., Lindquist, S.-E., Wang, L. and Muhammed, M., High light-to-enegy conversion efficiencies for solar cells based on nanostructured ZnO electrodes. *J. Phys. Chem.*, 1997, **101**, 2598–2601.
12. Keis, K., Vayssieres, L., Lindquist, S.-E. and Hagfeldt, A., Nanostructured ZnO electrodes for photovoltaic applications. *Nanostruct. Mater.*, 1999, **12**, 487–490.
13. BeeMann, N., Vayssieres, L., Lindquist, S.-E. and Hagfeldt, A., Photoelectrochemical studies of oriented nanorod thin films of hematite. *J. Electrochem. Soc.*, 2000, **147**, 2456–2461.
14. Izaki, M. and Ohmi, T., Electrolyte optimization for cathodic growth of zinc oxide films. *J. Electrochem. Soc.*, 1996, **143**, L53–L55.
15. Haga, K., Katahira, F. and Watanabe, H., Preparation of ZnO films by atmospheric pressure chemical-vapor deposition using zinc acetylacetonate and ozone. *Thin Solid Films*, 1999, **343**, 145–147.
16. Ambia, M. G., Islam, M. N. and Hakim, M. O., Effects of deposition variables on the spray pyrolysis of ZnO thin film. *J. Mater. Sci.*, 1994, **29**, 6575–6580.
17. Choi, J. H., Tabata, T. and Kawai, T., Initial preferred growth in zinc oxide thin films on Si and amorphous substrates by a pulsed laser deposition. *J. Cryst. Growth*, 2001, **226**, 493–500.
18. Izaki, M. and Ohmi, T., Transparent zinc oxide films prepared by electrochemical reaction. *Appl. Phys. Lett.*, 1996, **68**, 2439.
19. Vayssieres, L., Growth of arrayed nanorods and nanowires of ZnO from aqueous solutions. *Adv. Mater.*, 2003, **15**, 464–466.
20. Yamabi, S. and Imai, H., Growth conditions for wurtzite zinc oxide films in aqueous solutions. *J. Mater. Chem.*, 2002, **12**, 3773–3778.
21. Vayssieres, L., Keis, K., Lindquist, S.-E. and Hagfeldt, A., Three-dimensional array of highly oriented crystalline ZnO microtubes. *Chem. Mater.*, 2001, **13**, 4395–4398.
22. Vayssieres, L., Keis, K., Lindquist, S.-E. and Hagfeldt, A., Purpose-build anisotropic metal oxide material: 3D highly oriented micro array of ZnO. *J. Phys. Chem. B*, 2001, **105**, 3350–3352.
23. Liu, T. Q., Skurai, O., Mizutani, N. and Kato, M., Preparation of spherical fine ZnO particles by the spray pyrolysis method using ultrasonic atomization techniques. *J. Mater. Sci.*, 1986, **21**, 3698–3702.
24. Ohyama, M., Kozuka, H., Yoko, T. and Sakka, S., Preparation of ZnO films with preferential orientation by sol–gel method. *J. Ceram. Soc. Jpn.*, 1996, **104**, 296–300.